JOURNAL OF VIROLOGY, Apr. 1995, p. 2547–2556 Vol. 69, No. 4
0022-538X/95/$04.00+0

Mutations in the Helicase-Like Domain of Protein 1a Alter the Sites of RNA-RNA Recombination in Brome Mosaic Virus

PETER D. NAGY,[1] ALEKSANDRA DZIANOTT,[1] PAUL AHLQUIST,[2] AND JOZEF J. BUJARSKI[1]*

Plant Molecular Biology Center and Department of Biological Sciences, Northern Illinois University, De Kalb, Illinois 60115,[1] and Institute for Molecular Virology and Department of Plant Pathology, University of Wisconsin—Madison, Madison, Wisconsin 53706[2]

Received 2 August 1994/Accepted 12 January 1995

A system that uses engineered heteroduplexes to efficiently direct in vivo crossovers between brome mosaic virus (BMV) RNA1 and RNA3 (P. Nagy and J. Bujarski, Proc. Natl. Acad. Sci. USA 90:6390–6394, 1993) has been used to explore the possible involvement of BMV 1a protein, an essential RNA replication factor, in RNA recombination. Relative to wild-type 1a, several viable amino acid insertion mutations in the helicase-like domain of BMV 1a protein affected the nature and distribution of crossover sites in RNA3-RNA1 recombinants. At 24°C, mutants PK19 and PK21 each increased the percentage of asymmetric crossovers, in which the RNA1 and RNA3 sites joined by recombination were not directly opposite each other on the engineered RNA3-RNA1 heteroduplex used to target recombination but rather were separated by 4 to 85 nucleotides. PK21 and another 1a mutant, PK14, also showed increases in the fraction of recombinants containing nontemplated U residues at the recombination junction. At 33°C, the highest temperature that permitted infections with PK19, which is temperature sensitive for RNA replication, the mean location of RNA1-RNA3 crossovers in recombinants recovered from PK19 infections was shifted by nearly 25 bp into the energetically less stable side of the RNA1-RNA3 heteroduplex. Thus, mutations in the putative helicase domain of the 1a protein can influence BMV RNA recombination. The results are discussed in relation to models for recombination by template switching during pausing of RNA replication at a heteroduplexed region in the template.

The apparently modular evolution of positive-strand RNA viruses, natural sequence rearrangements in such viruses, and the presence of cellular sequence elements in some viral genomes (for reviews, see references 12, 14, 15, 20, 24, 31, and 34) all indicate an important role for recombination in RNA virus variation. Several lines of evidence suggest that recombination in RNA viruses can occur via a copy choice mechanism due to strand switching by viral RNA-dependent RNA polymerase (replicase) (20, 24). Possible pathways for recombination by template switching have been proposed for several positive-strand RNA viruses. For turnip crinkle virus, a promoter-like RNA element was suggested to facilitate reinitiation by replicase-nascent strand complexes that had dissociated from their original template RNA (8, 9). For brome mosaic virus (BMV), local heteroduplexes between viral RNAs were demonstrated to promote and direct recombination (6, 28, 29). Similar heteroduplex-mediated mechanisms have been suggested to be responsible for inserting bovine polyubiquitin mRNA sequences into bovine diarrhea virus RNA (26) and to facilitate intertypic recombination in poliovirus (30). Kirkegaard and Baltimore also provided genetic evidence for template switching in poliovirus recombination (21).

BMV is a tripartite RNA virus whose RNA3 encodes the 3a movement protein and the coat protein, which are involved in infection spread (27), while RNA1 and RNA2 encode proteins 1a and 2a, which are required for RNA replication (1). Recombination has been targeted between BMV RNA1 and RNA3 by inserting short, antisense RNA1 segments into RNA3 (29). Crossover sites in the resulting recombinants were clustered within or immediately to one side of the heteroduplex engineered between the parental RNA3 and RNA1 (29). This pattern of crossing over suggested that the recombinants might result from occasional template switching by the viral RNA replicase at the heteroduplex between RNA1 and RNA3, possibly because of difficulties in unwinding stable portions of the heteroduplex.

BMV RNA replication proteins 1a and 2a each share sequence conservation with nonstructural proteins of the animal alphaviruses and numerous plant RNA viruses. 2a contains a central conserved domain that likely represents the RNA polymerase catalytic unit (1, 22). 1a contains an N-terminal m^7G methyltransferase-like domain and a C-terminal helicase-like domain (1). This latter domain contains six conserved motifs related to known helicases (16), and mutations in or near these motifs abolish or perturb BMV RNA synthesis (23). 1a and 2a interact in vitro (19) to form a complex required for RNA replication in vivo (11), and the regions responsible for this 1a-2a interaction have been mapped (18). Consistent with the possible association of helicase and polymerase functions in a 1a-2a complex, BMV RNA-dependent RNA polymerase extracts show a significant, though not unlimited, ability to copy through double-stranded regions made by annealing portions of an RNA template to complementary cDNAs (2).

Together, the results cited above suggest that some BMV RNA recombination events might occur when the putative 1a helicase domain fails to carry out or pauses in its proposed role of unwinding duplex regions of the template to facilitate continued polymerase elongation (1). When progress on the original template is so impeded, the polymerase might sometimes have the opportunity to switch to copying the adjacent single-stranded region of a heteroduplexed RNA strand. Accordingly, in the experiments reported here, we examined the possible effects of mutations within the 1a helicase-like domain on the frequency or sites of heteroduplex-mediated recombination between BMV RNA1 and RNA3. The results revealed several effects of 1a mutations on recombination, including, for a temperature-sensitive (*ts*) 1a mutant, a temperature-dependent

* Corresponding author.

shift of crossovers toward the energetically less stable portions of the RNA1-RNA3 heteroduplex. Other non-*ts* 1a mutants showed different alterations in the distribution of recombination sites and/or increased incidence of nontemplated U residues at recombination junctions. Thus, consistent with recombination as a by-product of RNA replication, mutations in the BMV 1a RNA replication protein can influence the distribution of recombination sites between BMV RNAs.

MATERIALS AND METHODS

Materials. Plasmids pB1TP3, pB2TP5, and pB3TP7 (17) were used to synthesize infectious in vitro transcripts of wild-type (wt) BMV RNA1, RNA2, and RNA3. Plasmids pB1PK14, pB1PK19, and pB1PK21 (23) were used to synthesize BMV RNA1 transcripts bearing the PK14, PK19, and PK21 mutations, respectively. Plasmid pPN8(−) (29) was used to obtain transcripts of the PN8(−) derivative of BMV RNA3. Moloney murine leukemia virus reverse transcriptase, restriction enzymes, and T7 RNA polymerase were from GIBCO-BRL (Gaithersburg, Md.), and a Sequenase kit was from United States Biochemical Corporation (Cleveland, Ohio).

In vitro transcription, whole-plant infections, and RNA purification. Full-length, capped RNA transcripts were made from *Eco*RI-linearized plasmids according to previously published procedures (17). *Chenopodium quinoa* leaves were inoculated with a mixture of the transcribed BMV RNA components as described in reference 28. Briefly, a mixture of 1 μg of each transcript in 15 μl of inoculation buffer (10 mM Tris [pH 8.0], 1 mM EDTA, 0.1% celite, 0.1% bentonite) was used to inoculate one fully expanded leaf. In each experiment, six separate leaves were inoculated for each RNA1 mutant-temperature combination. Each such inoculation experiment was repeated two or three times. The inoculated *C. quinoa* plants were maintained in a growth chamber at either 24 or 33°C (the temperature was lowered by 2°C during the dark period for 10 h) for 2 weeks. Plants that were inoculated with PK19 did not produce any local lesions at 35 and 37°C. Local lesions were counted 14 days postinoculation, and for each RNA1 mutant-temperature combination, lesions selected at random were excised for RNA extraction. Total RNA was extracted from each local lesion, using phenol-chloroform extraction in a 1% sodium dodecyl sulfate–50 mM glycine–50 mM NaCl–10 mM EDTA (pH 9.0) buffer.

Amplification of recombinant RNA3s by RT-PCR, cloning, and sequencing. The 3′-proximal sequences in recombinant BMV RNA3 molecules were amplified with a reverse transcription-PCR (RT-PCR) procedure exactly as described in reference 28. Briefly, first-strand cDNA was synthesized in a 10-μl reaction mixture that contained 4 μl of the extract RNA, 1 mM each deoxynucleoside triphosphate (dNTP), 1 U of RNasin per μl, 25 pM first-strand synthesis primer (primer 1 [CAGTGAATTCTGGTCTCTTTTAGAGATTTACAG], which is complementary to the 3′-terminal 23 nucleotides [nt] of all of the BMV virion RNAs [3]), 50 mM KCl, 20 mM Tris-HCl (pH 8.4), 3 mM $MgCl_2$, and 200 U of Moloney murine leukemia virus reverse transcriptase. After incubation at 55°C for 40 min, the reverse transcriptase was heat inactivated at 95°C for 5 min, the volume was adjusted to 50 μl, and the mixture was subjected to PCR amplification. The PCR mixture contained 50 mM KCl, 20 mM Tris-HCl (pH 8.4), 1.5 mM $MgCl_2$, 1 mM each dNTP, 25 pM primer 1 (see above), 25 pM second-strand primer (primer 2 [CTGAAGCAGTGCCTGCTAAGGCGGTC], which corresponds to nt 367 to 392 from the 3′ end of wt BMV RNA3), and 1 U of *Taq* DNA polymerase (Perkin-Elmer). After 40 thermocycles (94°C for 1 min, 60°C for 1 min, and 72°C for 2 min), the resulting cDNA was analyzed in 1% agarose gels. The use of primer 1 created an *Eco*RI site (underlined) at the 3′ end of the cDNA products. The resulting cDNA products were digested with restriction enzymes *Eco*RI and *Xba*I and ligated between the corresponding sites in the polylinker of the pGEM3zf(−) cloning vector (Promega). The sites of crossovers between RNA3 and RNA1 in the recombinants were determined by sequencing with the Sequenase kit (U.S. Biochemical) according to the manufacturer's specifications.

Stability of 1a mutants in *C. quinoa*. The 3′-half sequences of wt, PK14, PK19, and PK21 RNA1s obtained from eight separate local lesions of *C. quinoa* 14 days after inoculation were amplified by RT-PCR using primers 1 (see above) and 3 (5′-GACCAAGCTTCGAAGAAGAAGGCG-3′, corresponding to positions 1583 to 1607 of wt RNA1). Conditions of RT-PCR were the same as described above except that reverse transcription was performed at 37°C and the parameters for PCRs were as follows: 94°C for 1 min, 55°C for 1 min, and 72°C for 3 min. After 40 thermocycles, the PCR products were purified by phenol-chloroform extraction and ethanol precipitation. Restriction enzyme digestion of the resulted PCR products with either *Bam*HI (for PK19 and PK21) or *Apa*I (for PK14) was used to demonstrate the presence of the corresponding linker sequences in the progenies of the particular RNA1 mutants.

Analysis of growth characteristics of selected RNA3 recombinants by Northern (RNA) blotting. Full-length cDNA clones of two unusual recombinants derived from PK19 infections (marked by triangles in Fig. 3) were generated by replacing the 3′-terminal *Xba*I-*Eco*RI fragment of wt RNA3 cDNA clone pB3TP7 with the corresponding *Xba*I-*Eco*RI fragments derived from the cloned partial cDNAs of the particular recombinant (see above). In vitro-transcribed RNA3 transcripts representing sequences of the selected recombinants were used together with one of the RNA1s (wt, PK14, PK19, and PK21) and wt RNA2 to inoculate leaves of *C. quinoa*. After inoculation, plants were incubated at 24 or 33°C. Total RNA extracts were prepared as described above from four separate local lesions for each mutant RNA1-recombinant RNA3 combination 14 days after inoculation. One-tenth of each total RNA extract was used for 1% agarose gel electrophoresis; this procedure was followed by a transfer to a nylon membrane (Hybond N+; Amersham) and hybridization to a ^{32}P-radiolabeled BMV RNA positive-strand-specific probe under the conditions described by Kroner et al. (22).

Statistical analyses. For the distribution of crossover sites observed for each mutant-temperature combination, the mean recombination site and the standard deviation about that mean were calculated by using computer program SuperANOVA (Abacus Concepts, Inc.) run on a Macintosh computer. To assess whether the distribution of crossover sites differed significantly between any two mutants, the same program was used to apply the Duncan new multiple-range procedure (13). This procedure utilizes an algorithm which makes all pairwise comparisons of the means by ordering them from smallest to largest and then uses the expected mean square values, the sample size from each group, the level of significance, and tabulated values of the Duncan statistics to compute critical ranges. These ranges are thereafter compared with the differences between the ordered means to identify which means are significantly different from any others (33).

RESULTS

To test whether mutations in a BMV-encoded protein required for RNA replication could influence RNA-RNA recombination, we examined three viable 1a mutants, designated PK14, PK19, and PK21 (Fig. 1A). Each of these mutants has a two-amino-acid insertion within the helicase-like domain of 1a. As reported previously (23), PK14 and PK21 do not cause any conspicuous changes in BMV RNA replication in barley protoplasts. By contrast, PK19 is *ts*, supporting a wt level of BMV RNA replication at 24°C but no RNA synthesis at 35°C.

To target recombination events between BMV RNA1 and RNA3, we used a previously described RNA3 derivative, designated PN8(−) (29). As illustrated in Fig. 1A, PN8(−) RNA3 contains a long, chimeric 3′ noncoding region that serves two purposes. First, to promote recombination with RNA1, PN8(−) RNA3 contains a 141-nt-long antisense RNA1 sequence, inserted immediately 3′ to the coat protein open reading frame (region bounded by dotted lines in Fig. 1A). This antisense RNA1 insert, which is punctuated at its 5′ end by three regions of mismatch with RNA1, enables PN8(−) RNA3 to form an imperfect heteroduplex with RNA1 (Fig. 1B) that resembles the imperfect double-stranded regions in proposed recombination intermediates between wt BMV RNAs (6, 28, 29). As shown previously (29), when cells are infected with wt RNA1, wt RNA2, and PN8(−) RNA3, these features lead to the high-frequency appearance of recombinant variants of RNA3, in which crossing over within the region of the Fig. 1B heteroduplex has replaced the 3′-proximal segment of PN8(−) RNA3 with that from RNA1. Since the 3′-terminal 200 nt of all BMV RNAs are almost perfectly conserved, such recombinants are fully competent for replication.

Second, the extreme 3′-terminal sequences of PN8(−) RNA3 following the antisense RNA1 insert contain BMV sequences essential for directing negative-strand RNA synthesis. However, this region also bears a previously described (29) set of deletions, duplications, and insertions that cause PN8(−) RNA3 to replicate and accumulate more poorly than either wt RNA3 or the heteroduplex-mediated recombinants in which these debilitated PN8(−) 3′ sequences are replaced by the wt 3′ noncoding sequences of RNA1. Thus, the heteroduplex-mediated PN8(−)-RNA1 recombinants have a selective replicative advantage over the parental PN8(−) RNA3, facilitating their detection and recovery.

Recombination assays with wt and mutant 1a genes. Leaves of *C. quinoa*, a local lesion host for BMV, were inoculated with

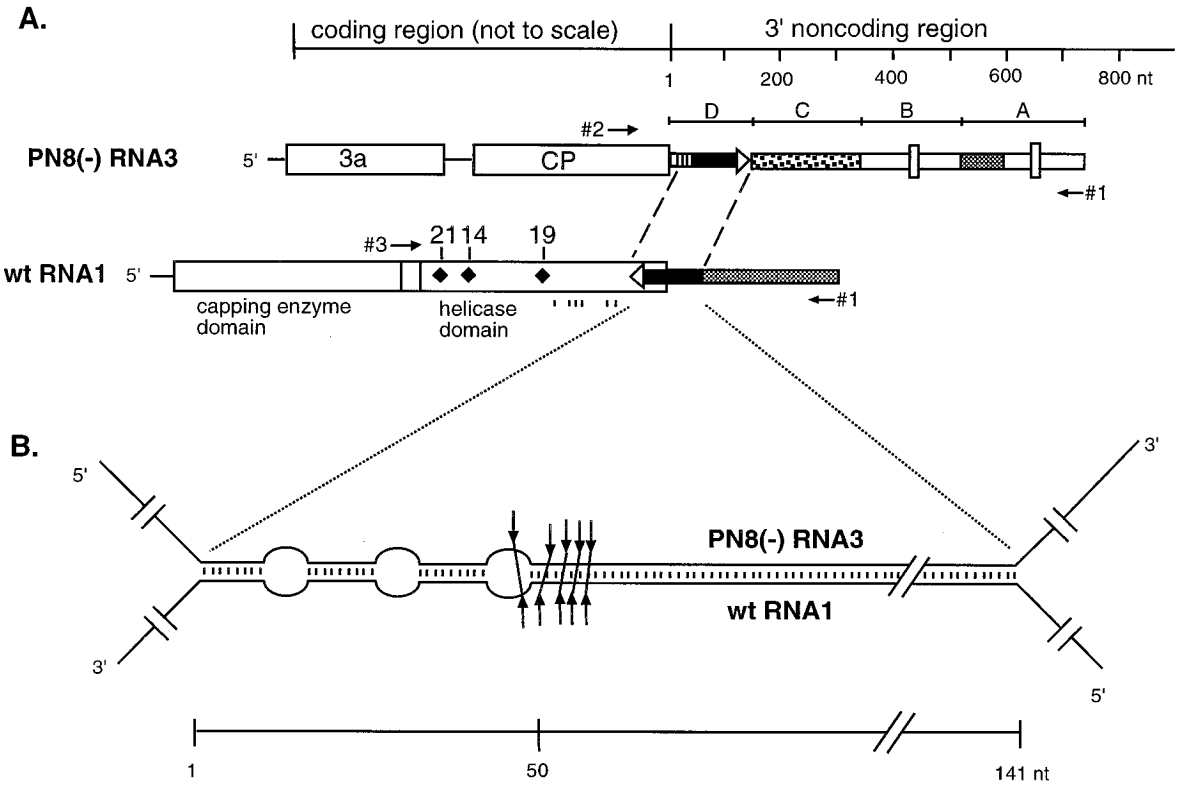

FIG. 1. (A) Schematic representation of the structure of the PN8(−) BMV RNA3 derivative and the locations of insertion mutations in BMV RNA1. As previously described (29), the 3′ noncoding sequence of the PN8(−) RNA3 mutant consists of four segments shown as regions A to D. The extreme 3′ segment A is a functional chimera derived from the 3′ ends of RNA1 (positions 163 to 236 from the 3′ end [3]) and RNA3 (positions 1 to 162 from the 3′ end). Segment B is derived from the 3′ noncoding region of RNA3 with a deletion of 6 nt at the very 3′ end (positions 7 to 200). In addition, both elements A and B contain the same 20-nt deletion between nt 81 and 100 (symbolized by vertical open rectangles). Segment C (stippled sequence) contains a 197-nt sequence derived from the 3′ noncoding terminus of cowpea chlorotic mosaic virus RNA3 without the 3′ proximal 23 nt (positions 24 to 220 [4]). Because segments B and C lack the extreme 3′ ends of their parental RNAs, RNA replication initiates exclusively from the 3′-terminal BMV sequence of segment A (29). Segment D consists of a 141-nt-long RNA1-derived sequence (marked by a horizontal filled-boxed arrow on the right) inserted in reverse orientation (the head of the arrow shows the orientation) to facilitate the formation of local heteroduplexes with wt RNA1 (see panel B). Three sequence mismatches (shown by three open boxes inside segment D) were introduced into the 141-nt reverse RNA1 insert in PN8(−) RNA3 in order to cause the crossovers to occur at more inner parts of the heteroduplex (see text and reference 29). The locations of the oligonucleotide primers used for PCR are shown by short horizontal arrows denoted 1 and 2 beneath and above the PN8(−) map and 3 above the RNA1 map. Primer 1 also anneals to the 3′ terminus of RNA1 and RNA2. CP, coat protein. (B) Proposed schematic structure of the heteroduplex formed between the antisense region of PN8(−) RNA3 and the complementary region of RNA1. The diagram shows the two positive-strand BMV RNA molecules (represented by thick lines), which are arranged in opposite orientations and hybridized within the centrally located double-stranded region. Three bubbles at the left side of the heteroduplex symbolize unhybridized mismatch regions. The region within which most of the observed crossovers occurred is marked by vertical arrows. The lengths of the heteroduplex region and other elements can be estimated by nucleotide positions above the PN8(−) RNA3 line.

a mixture of in vitro-transcribed RNA1 (either wt or one of the PK mutants), wt RNA2, and PN8(−) RNA3. To analyze whether the *ts* mutant PK19 had a *ts* phenotype in recombination, half of the inoculated plants were kept at 24°C and half were kept at 33°C. As an initial assay for recombination, individual local lesions were excised from the inoculated leaves at 14 days postinoculation, total RNA was isolated separately from each lesion, and the 3′ noncoding regions of the RNA3 progeny were amplified by RT-PCR, electrophoresed in agarose gels, and visualized by ethidium bromide staining as described in Materials and Methods. The first-strand cDNA primer was complementary to the extreme 3′ sequence conserved on all BMV RNAs, while the second-strand primer corresponded to a sequence within the BMV coat protein gene, making the PCR reaction specific for RNA3 derivatives (Fig. 1A). The PCR product so amplified for the parental PN8(−) RNA3 (Fig. 1A) was 860 nt in length, while RNA3 recombinants produced by crossovers between PN8(−) RNA3 and RNA1 within the region of their complementarity (Fig. 1B) gave rise to smaller PCR products due to replacement of the long 3′ noncoding region of PN8(−) (743 nt) with the shorter 3′ noncoding region of RNA1 (274 nt). Consistent with such recombination, a major PCR product smaller than 860 nt was found in 84 to 88% of lesions from inoculations involving wt RNA1 and 100% of lesions from inoculations with PK14, PK19, and PK21 RNA1 mutants (Table 1). The sizes of these products varied from approximately 350 to 525 nt among different lesions (Fig. 2). Despite this variation among different lesions, 95% of recombinant-containing lesions each contained only a single major type of recombinant RNA3, as determined by agarose gel electrophoresis and subsequent cloning of the RT-PCR products and sequencing of at least five clones per lesion in preliminary experiments. Only one lesion of those in Fig. 2 accumulated significant levels of two recombinants (Fig. 1A, lane 16). The 860-nt PCR band corresponding to the parental PN8(−) RNA3 was also detected in approximately 30% of all recombinant-containing lesions, usually as a weaker, more slowly migrating band accompanying a stronger recombinant PCR product (Fig. 2).

To test for possible RT-PCR-dependent recombination or other PCR artifacts, a sample of each inoculum mixture [containing wt or mutant RNA1, wt RNA2, and PN8(−) RNA3

TABLE 1. Characterization of crossover sites obtained from infections with three BMV 1a protein mutants

Mutant	Treatment (°C)	No. of clones sequenced[a]	% Incidence of:		
			Recombination[b]	Nontemplated nucleotides[c]	Significantly asymmetric crossovers[d]
wt	24	25	84	8 ± 1	16
PK14	24	23	100	22 ± 2	22
PK19	24	34	100	6 ± 1	50
PK21	24	26	100	27 ± 2	35
wt	33	25	88	4 ± 1	8
PK14	33	22	100	5 ± 1	14
PK19	33	27	100	0	11
PK21	33	25	100	8 ± 2	24

[a] Each clone represents an independent RNA3-RNA1 recombinant isolated from a separate local lesion.
[b] Percentage of lesions that contained recombinant RNA3 molecules as determined by size fractionation of RT-PCR products by agarose gel electrophoresis.
[c] Percentage of recombinants that contained nontemplated nucleotides at the crossover sites. Standard deviations were calculated from the analysis of recombinants isolated from 12 leaves (one to three lesions per leaf).
[d] Percentage of recombinants that had the PN8(−) RNA3 site more than 3 bp away from the RNA1 site on the heteroduplex formed between complementary regions of PN8(−) RNA3 and RNA1 (see Fig. 3).

transcripts] was subjected to RT-PCR with the same primers and conditions used to test total nucleic acid extracts from *C. quinoa* local lesions. In these control reactions, the expected 860-nt band corresponding to PN8(−) RNA3 was always the only RT-PCR product observed (Fig. 2B, lane Φ). As another control, multiple independent PCR amplifications were sometimes performed on the cDNA products derived from a single local lesion. Such PCR reactions always reproducibly amplified a common recombinant species, while, as noted above, PCR amplifications of cDNAs from different lesions produced products of various sizes. Together, these results ruled out the possibility that the observed PN8(−)-RNA1 recombinants were generated during RT-PCR rather than during BMV infection.

To determine whether the 1a gene linker insertion mutations were maintained during the formation of recombinant RNA3s, we tested the stability of the RNA1 mutations during infection. The 3′ half of RNA1, which includes all three mutations (Fig. 1A), was amplified by RT-PCR with primers 1 and 3. The same total RNA extracts of *C. quinoa* were used for these studies as for the recombinant RNA3 studies (see above). The presence of the inserted *Bam*HI or *Apa*I linker sequences was demonstrated for eight separate samples in each mutant RNA1-recombinant RNA3 combination by restriction enzyme digestion (*Bam*HI for PK19 and PK21 and *Apa*I for PK14). Similar to control results obtained in parallel reactions with mixtures of in vitro-transcribed RNA1 (either wt, PK14, PK19, or PK21), RNA2, and RNA3, we found that the RT-PCR-amplified RNA1-specific PCR products were cut by the appropriate restriction enzyme (to 95 to 100% completeness; results not shown). This finding demonstrates that 1a gene mutations were stably maintained during infection for all three PK*n* mutants and that any possible 1a revertants that might have emerged remained at most minor species in the infection.

Effect of mutations in the 1a helicase-like domain on the distribution of crossover sites. To compare the distributions of crossover sites in the presence of wt and mutant 1a genes, the PCR-amplified, RNA3-specific cDNA products were cloned into a suitable plasmid and sequenced as described in Materials and Methods. To provide a representative distribution of crossover sites for comparison, 22 to 34 clones were sequenced for each RNA1 mutant-temperature combination. To ensure that each sequence represented an independent recombination

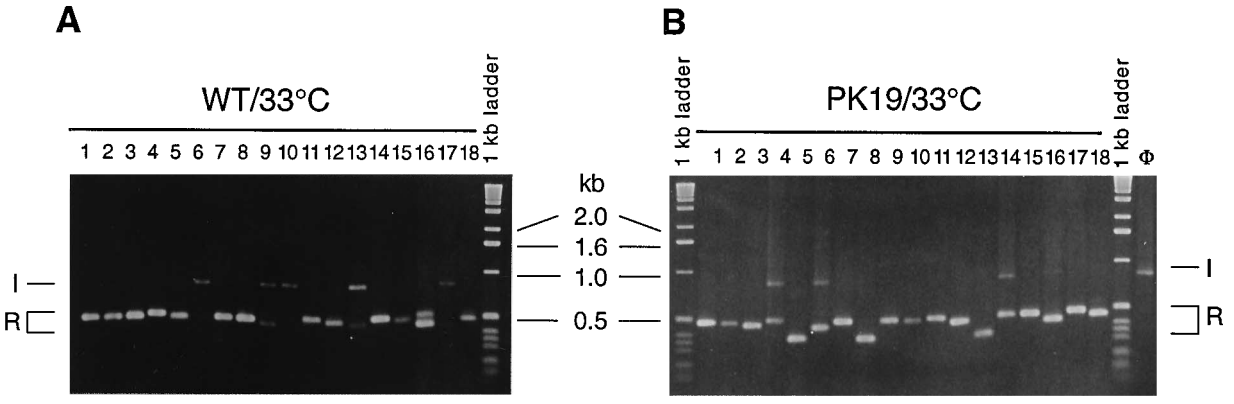

FIG. 2. Characterization of BMV RNA3 recombinants by agarose gel electrophoresis of RNA3-specific PCR products obtained by RT-PCR using primers 1 and 2 (as specified in Fig. 1A) from total RNA preparations extracted from individual local lesions as described in Materials and Methods. The RT-PCR products of progeny RNA3 derived from 18 separate local lesions that were obtained from either wt (A) or PK19 (B) RNA1 infection at 33°C are shown. Lane Φ shows a control RT-PCR amplification that was performed by using a mixture of in vitro-transcribed wt RNA1 and RNA2 and PN8(−) RNA3. Positions of PCR products corresponding to the length of the inoculated PN8(−) RNA3 (I) and of the newly emerged recombinants (R) are shown. The sizes of PCR products can be estimated by comparison with a standard 1-kb DNA ladder (GIBCO-BRL) shown in lanes marked 1 kb ladder. Note the homogeneity of RT-PCR products within the samples and their size variation among the samples.

event, each clone was derived from an independent local lesion. This approach was judged to be the most productive since, as noted above, 95% of the recombinant-containing lesions had a single major recombinant species.

The sequencing confirmed that the PCR products smaller than 860 nt represented recombinants between PN8(−) and RNA1. Recombination invariably occurred within or immediately adjacent to the region of engineered complementarity between the two starting RNAs (Fig. 1B). Figure 3A shows the distributions of crossover sites observed for infections at 24°C involving the wt 1a gene or mutants PK14, PK19, and PK21. For PK14 and wt 1a, the crossover distributions observed at 24°C were quite similar (Fig. 3A). For both, the majority of crossovers clustered between 50 and 70 nt from the left side of the heteroduplex portrayed in Fig. 3A. Also, a similar recombination hot spot was observed with both wt 1a and PK14, represented by seven and nine crossovers, respectively, that occurred 62 to 63 nt from the left side of the heteroduplex. For these and most other wt and PK14 recombinants, the crossover sites on PN8(−) RNA3 and RNA1 were aligned within 0 to 3 nt of each other on the illustrated heteroduplex; hereafter, such crossovers will be referred to as symmetric. The remaining recombinants (16% for wt and 22% for PK14) resulted from asymmetric crossovers linking PN8(−) and RNA1 sequences that were widely separated on the heteroduplex. Among nine asymmetric recombinants recovered from infections with wt 1a or PK14 at 24°C, seven had the crossover site on PN8(−) RNA3 (upper strand in Fig. 3A) displaced in the 3′ direction along PN8(−) from the crossover site on RNA1, while two had crossover sites in the opposite orientation.

Unlike the case for PK14, the crossover distributions resulting from PK19 and PK21 infections showed significant differences from wt 1a infections. At 24°C, the incidence of asymmetric crossovers was significantly increased, to 35% of total recombinants for PK21 and to 50% for PK19, versus 16% for wt 1a (Fig. 3A and Table 1). Moreover, the average separation between PN8(−) and RNA1 crossover endpoints in asymmetric crossovers was much greater for PK19 and PK21 than for wt 1a or PK14 (Fig. 3A). The most asymmetric PK19 crossovers, e.g., joined PN8(−) and RNA1 sites separated by up to 85 nt in the heteroduplex.

The differences in crossover distributions between wt 1a and the 1a mutants might reflect differences in either the generation or subsequent viability of different types of recombinants. To investigate if the most unusual recombinant RNA3s observed in mutant 1a backgrounds were viable in the wt 1a background, we constructed full-length cDNA clones of two of the most unusual RNA3 recombinants that were found only in PK19 infections and tested their growth characteristics in infections involving wt and mutant 1a genes. One of the two recombinant RNA3s was recombinant 1 (marked by a triangle in the *ts* PK19B sequence in Fig. 3A), which contained an unusually long 3′ noncoding region (~420 nt) resulting from an asymmetric crossover. The other selected recombinant RNA3 was recombinant 5 (marked by a triangle in the *ts* PK19 sequence in Fig. 3B). This recombinant had a very short 3′ noncoding region (~250 nt) resulting from a crossover on the left side of the putative heteroduplex. In vitro-transcribed RNA1 (wt, PK14, PK19, or PK21), wt RNA2, and one of the selected recombinant RNA3s were used to inoculate leaves of *C. quinoa*. The inoculated plants were incubated either at 24 or 33°C for 2 weeks. Northern blot analysis with a BMV-specific RNA probe of total RNA extracts made from separate local lesions was used to determine the accumulation of progeny RNAs. Figure 4A shows that both recombinant RNA3s were viable and accumulated to very similar levels in wt, PK14, PK19, and PK21 infections at room temperature (lanes 1 to 8). Recombinant 1 accumulation at 33°C was lower than that at 24°C but comparable in wt, PK14, and PK21 infections (Fig. 4B, lanes 9, 10, and 12) and actually greater than recombinant 1 accumulation in PK19 infections (lane 11). At 33°C, recombinant 5 accumulation was not easily visible on the Northern blots in any of the infections (Fig. 4B, lanes 13 to 16). However, RT-PCR analysis with primers 1 and 2 demonstrated that recombinant 5 was present in local lesion infections with either wt or one of the PK*n* RNA1 derivatives (Fig. 4C, lanes 21 to 27). These data demonstrated that two of the most unusual recombinant RNA3s derived from PK19 1a infections were equally viable in infections with a wt, PK14, or PK21 1a gene. Thus, these results argue that the unusual recombinant RNA3s would have been observed if they had been generated in infections with any of these RNA1 derivatives. Taken together, the observed differences in the nature of recombinants are unlikely to result from differences in postrecombination selection.

Comparison of average crossover sites on RNA3 and RNA1. While Fig. 3A reveals some notable differences between the crossover distributions associated with wt 1a and the PK19 and PK21 mutants, the raw data in the Fig. 3 crossover distributions are complex. Therefore, it was also useful to apply some simpler measures for objectively comparing the distributions. To this end, the mean positions and standard deviations of crossover endpoints on both PN8(−) RNA3 and RNA1 were plotted for infections with wt 1a and each 1a mutant. This display (Fig. 5) makes the major conclusions from Fig. 3A even more apparent. For wt 1a infections at 24°C, the average crossover endpoints on PN8(−) RNA3 (upper strand) and RNA1 (lower strand) were immediately adjacent to each other in the heteroduplex, at residues 62 and 61, respectively. The positions of the average crossover endpoints in PK14 infections were similar to those for the wt; i.e., they were separated from the wt values by less than half of the standard deviation of either distribution. In contrast, for PK19 infections at 24°C, the average crossover endpoints on RNA3 and RNA1 were markedly shifted away from each other toward the extremes of the heteroduplex, leaving a 19-nt gap reflecting the crossover asymmetry apparent for PK19 in Fig. 3A. PK21 infections at 24°C produced a pattern intermediate between those of wt 1a and PK19, with a 10-nt gap between the average crossover sites on RNA3 and RNA1 (Fig. 5). Relative to infections with wt 1a, the PK21 pattern reflected primarily a leftward shift in the crossover endpoint on RNA1.

Effect of 1a mutation PK19 at 33°C. The effect of the *ts* PK19 mutant on recombination was also compared with effects of wt 1a and the other 1a mutants in infections at 33°C, the highest temperature at which PK19 RNA1, wt RNA2, and PN8(−) RNA3 produced local lesions on *C. quinoa*. For wt 1a and each of the three mutants, the incidence of asymmetric crossovers declined significantly at 33°C versus 24°C (Fig. 3 and Table 1). At 33°C, most of the crossovers seen in infections with wt 1a, PK14, and PK21 clustered between positions 60 and 70 on the heteroduplex map of Fig. 3B. PK19, however, differed from wt 1a and the other 1a mutants in having a much higher incidence of crossovers in the left half of the heteroduplex, including several recombination hot spots leftward of position 60. One of these recombination hot spots was located several nucleotides immediately to the left of the heteroduplex (Fig. 3B). Under the template switching model, these recombinants would result from crossovers that occurred before the polymerase active site entered the heteroduplex region (see Fig. 1B and Discussion).

The magnitude of the leftward shift in recombination sites in PK19 infections at 33°C is particularly clear in Fig. 5, where the

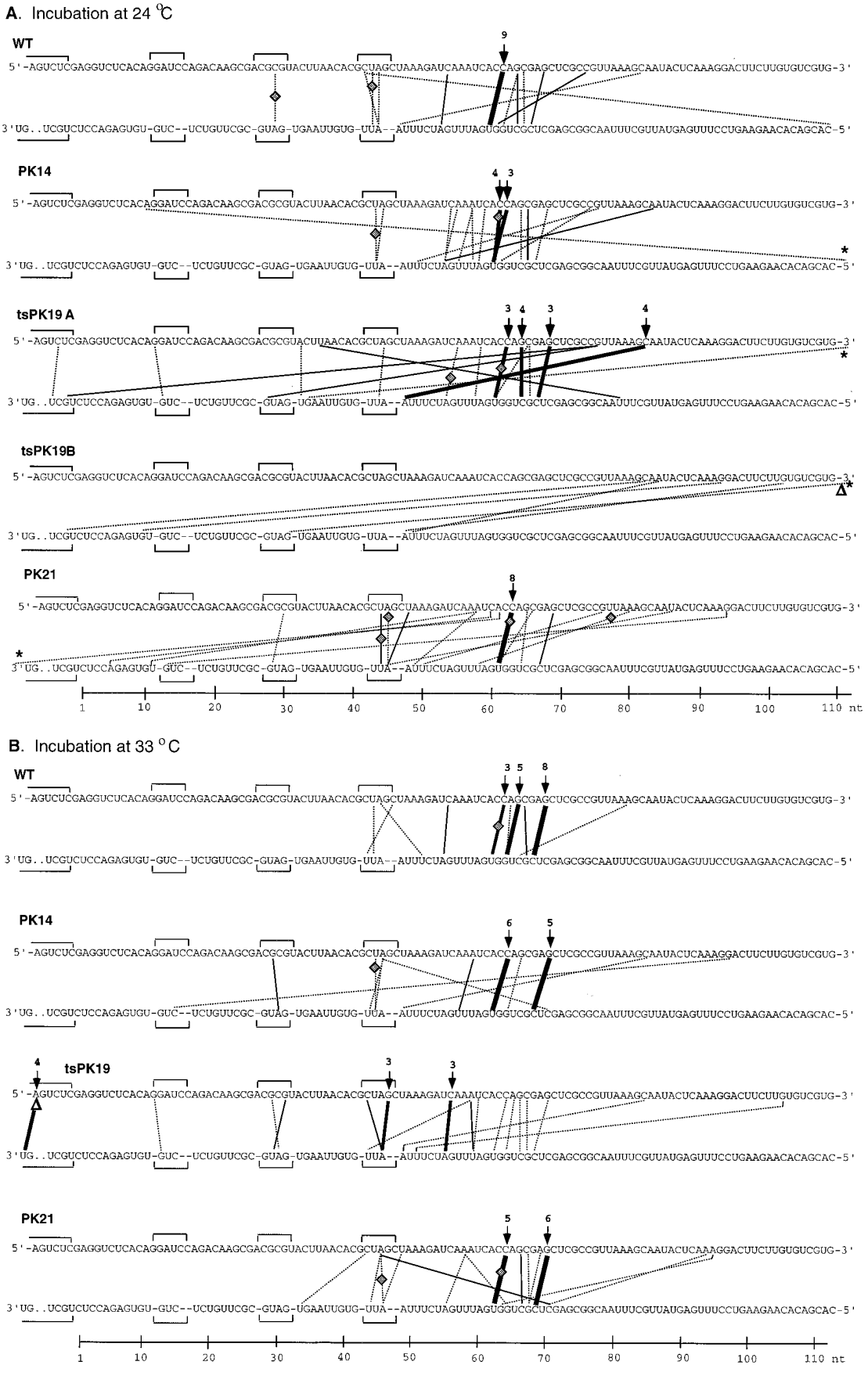
A. Incubation at 24 °C
WT
PK14
tsPK19 A
tsPK19B
PK21
B. Incubation at 33 °C
WT
PK14
tsPK19
PK21
1 10 20 30 40 50 60 70 80 90 100 110 nt

FIG. 3. Distribution of crossover sites observed for infections at 24°C (A) and 33°C (B) on the heteroduplexes formed between positive strands of RNA1 and PN8(−) RNA3 molecules. Upper lines represent the segment D region (antisense RNA1 sequences) of the positive strand of PN8(−) RNA3; lower lines represent the corresponding sense sequences on the positive strand of RNA1 (see also Fig. 1B). For each recombinant, the last nucleotide of PN8(−) RNA3 sequence preceding the recombination junction and the first nucleotide of RNA1 sequence following the recombination junction are connected by lines between the two RNA sequences. The thickness of each line is proportional to the number of independent lesions on *C. quinoa* that contained that particular recombinant; broken lines indicate crossovers that were identified only once, thin solid lines depict crossovers occurring twice, and the thickest lines represent those identified in three or more local lesions (as indicated by arrows with numbers above). Those crossovers containing nontemplated nucleotides are depicted by diamonds (the number of recombinants that contained nontemplated nucleotides at a particular crossover site and the inserted nucleotides are listed in Table 2). Horizontal brackets depict unpaired regions. The two dots at the left side of RNA1 represents the sequence 3′-UCCCGAGAGGAGC-5′ (not shown). Because a high number of asymmetric recombinants were obtained for the PK19 mutant at 24°C, the distribution of the corresponding crossovers is shown, for clarity, in two separate drawings (tsPK19A and tsPK19B). In panel A, the complete junction sites for four highly asymmetric recombinants (marked by asterisks) could not be displayed because of space limitations. They were located 103 nt upstream on RNA1 (PK14) or 6 (PK19A), 6 (PK19B), and 2 (PK21) nt downstream of the displayed nucleotides of PN8(−) RNA3 and RNA1, respectively. The two unusual recombinant RNA3s selected for examining their growth characteristics with wt or mutated 1a proteins (see Fig. 4) are marked with triangles.

mean positions of crossover sites are plotted for wt 1a and each mutant. At 33°C, the mean positions of crossover sites on PN8(−) RNA3 and RNA1 were quite similar between wt 1a, PK14, and PK21 and also similar to the mean positions found for wt 1a and PK14 at 24°C. However, in 33°C infections with PK19, the average positions of crossover sites on both PN8(−) RNA3 and RNA1 were shifted dramatically to the left relative to wt 1a or the other 1a mutants. As can be seen from Fig. 5, the 16-nt shift of the PK19 mean crossover positions relative to wt 1a represents a difference of almost 3 standard deviations in the crossover distribution. Use of the Duncan new multiple-range test (see Materials and Methods) confirmed that the crossover patterns induced by PK19 differed from those obtained with PK14, PK21, and wt viruses at a high probability level of 0.01.

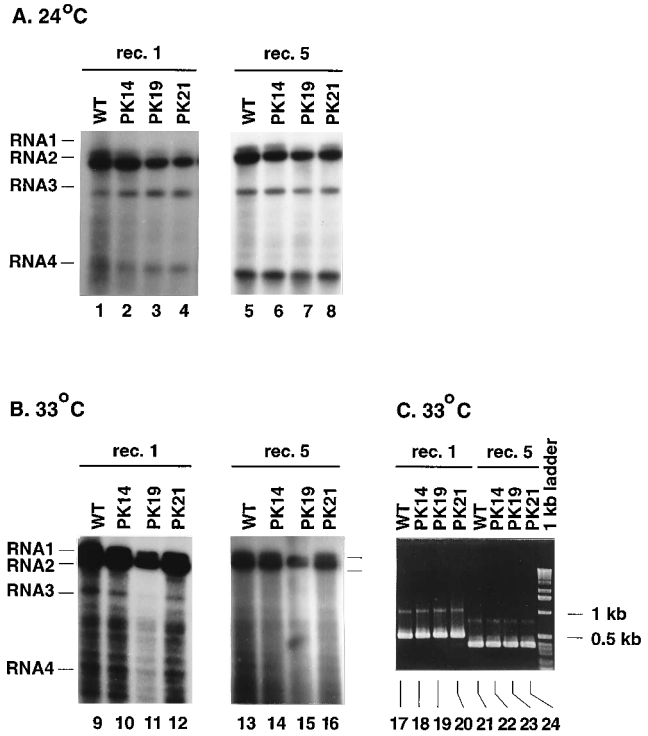

FIG. 4. Growth characteristics of two of the most unusual recombinant RNA3s in mutant and wt 1a backgrounds. Leaves of *C. quinoa* were inoculated with a mixture of in vitro-transcribed wt or PK*n* RNA1 (as shown above the lanes), wt RNA2, and recombinant 1 (rec. 1; marked by a triangle in the *ts* PK19B sequence in Fig. 3A) or recombinant 5 (rec. 5; marked by a triangle in the *ts* PK19 sequence in Fig. 3B) RNA3. Plants were incubated either at 24°C (A) or 33°C (B). Total RNA extracts were isolated and separated by electrophoresis on a 1% agarose gel. The RNA was transferred to a nylon membrane and probed with a 200-nt-long ^{32}P-labeled RNA probe specific for the 3′ noncoding region of RNA1 to RNA4. Some of the Northern blots were overexposed to visualize the less abundant RNA1 or RNA3. The total RNA extracts were also analyzed by RT-PCR with primers 1 and 2 in the 33°C experiments in order to show the presence of RNA3s in the local lesions (C).

Incorporation of nontemplated nucleotides. As found in an earlier study using the targeted recombination system (29), the RNA3-RNA1 recombination junctions of some recombinants (illustrated in Fig. 3 by the crossovers marked with a diamond) contained one or more additional nucleotides not present in the parental RNA1 or RNA3 sequences at the site of the crossover. For each RNA1-temperature combination, the percentage of crossovers bearing such apparently nontemplated nucleotides is shown in Table 1, and the actual sequences at these sites are given in Table 2. As shown in Table 2, the number of nontemplated nucleotides found in such recombinant junctions ranged from one to five, and with the exception of a single A residue, all of the nontemplated nucleotides were U residues. At 24°C, the frequency of recombinants with such junctions ranged from 6 to 8% (for wt and PK19) to 22 to 27% (for PK14 and PK21). Thus, although the distribution of crossover sites for PK14 did not differ appreciably from that of wt 1a (Fig. 3A), a higher incidence of nontempated nucleotide additions was associated with the PK14 infections (Table 2). At 33°C, the frequency of junctions with nontemplated nucleotides was reduced relative to 24°C for wt RNA1 and all three RNA1 mutants. At both temperatures, the junctions of recombinants bearing nontemplated nucleotides were not randomly distributed across the heteroduplex region. Rather, 17 of 20 examples observed in this study were clustered at or immediately adjacent to two nearly symmetric crossover sites designated A and B in Table 2. These sites correspond to crossovers at positions 44 and 45 (site A) or 62 and 63 (site B) in the heteroduplex mapped in Fig. 3.

DISCUSSION

The results presented in this paper report for the first time that a mutation in a viral protein involved in RNA replication affects the nature of RNA recombination products, thus providing crucial support for the idea that RNA recombination occurs during RNA replication. To examine the possible involvement of the virus-encoded RNA replicase components in genetic recombination in BMV, we used viable two-amino-acid-insertion mutations within the helicase-like domain of the BMV 1a protein. The recombination system used, in which crossing over occurred at regions of strong complementarity between the recombining RNAs, suggested the modification of the 1a helicase domain. We reasoned that if BMV replicase is involved in recombination, changes in the helicase-like C-terminal domain of 1a protein might affect recombination characteristics. In keeping with this expectation, statistically significant effects of 1a mutations on the location of crossover sites

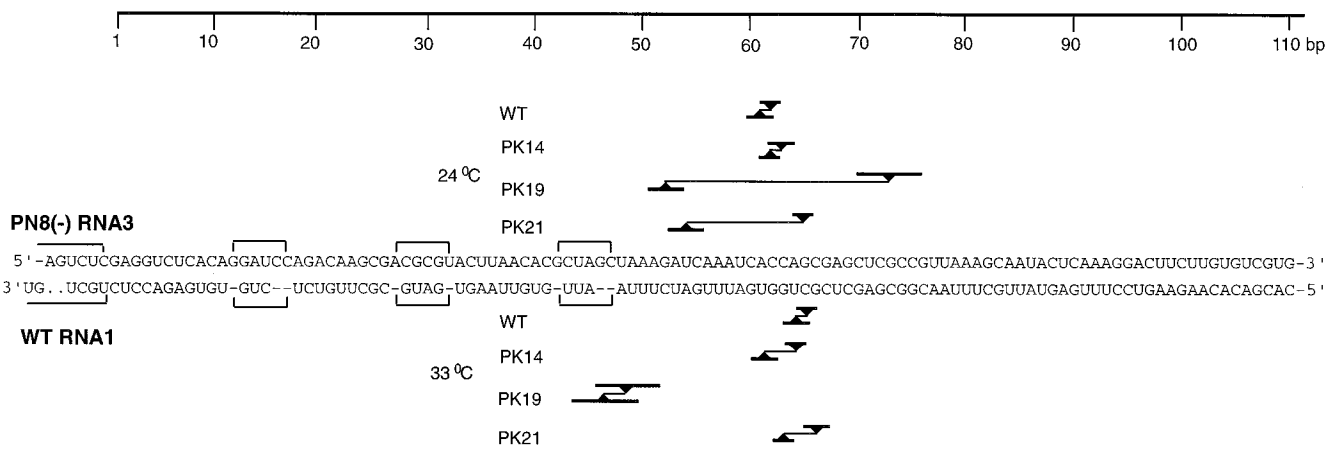

FIG. 5. Locations of the mean positions of crossover sites in recombinants obtained with the mutant and wt viruses (indicated on the left) at 24°C and 33°C. The nucleotide sequences forming the imperfect heteroduplex between PN8(−) RNA3 (upper sequence) and RNA1 (lower sequence) are displayed in the center. The mismatched regions in the heteroduplex are enclosed by three pairs of brackets. The mean crossover positions on PN8(−) RNA3 and wt RNA1 are depicted by pairs of connected arrowheads facing down and up, respectively. The horizontal bars at each arrowhead indicate the standard deviation from the mean for each distribution. The scale on the top shows the number of base pairs within the heteroduplex, counting from the left side.

and on the incorporation of nontemplated nucleotides were observed. More detailed aspects of the 1a mutant results and their relationship to the mechanism of recombination in BMV are discussed below.

Involvement of the 1a helicase domain in RNA recombination. The ability of 1a mutations to affect the positions of recombination sites was demonstrated in several ways. First, a leftward shift of crossovers on the heteroduplex in PK19 recombinants at 33°C, compared with wt recombinants, was observed. Such a shift was not found for PK14 and PK21 recombinants at the same temperature. The observed shift originated mainly because of the appearance of new recombination hot spots outside the heteroduplex and within the less stable left portion of the heteroduplex. By contrast, crossover sites that constituted recombination hot spots for wt, PK14, and PK21 at 33°C were found infrequently among PK19 recombinants. Additionally, an increased appearance of asymmetric crossovers that had the RNA1 and PN8(−) RNA3 junction sites far apart on the heteroduplex was more characteristic for PK19 and PK21 recombinants at 24°C than for other temperature-mutant combinations.

Because of the considerable distance in RNA1 between the sites of the 1a mutations and the region involved in the formation of the heteroduplex with PN8(−) RNA3, the effect of the mutations on recombination is likely to be in *trans*, through the 1a protein, rather than in *cis*, through any alteration in the heteroduplex structure. The observed differences also appear unlikely to result from differences in postrecombination selection. A large variety of recombinants that differed from one another by the positions of crossovers as well as the length of the 3′ noncoding region was observed in each RNA1 mutant-temperature combination. Thus, the accumulation of recombinants containing wildly variable 3′ noncoding sequences was permitted in each mutant-temperature combination.

The ability of mutations in a viral RNA replication protein to affect recombination is consistent with the popular view that some if not many RNA recombination events may occur as a by-product of viral RNA synthesis. A previously described tem-

TABLE 2. Nucleotide sequences at crossover sites in recombinants containing nontemplated nucleotide inserts

Recombinant	Mutant, temp (°C)	Sequence, RNA3/nontemplated/RNA1[a]	Group[b]	No. of independent isolations[c]
1	wt, 24	ACACGCU/**U**/UUGUGUU	A	1
2		GCGACGC/**UUUUU**/AUGCGCU	U	1
3	PK14, 24	AAAUCAC/**U**/UGAUUUG	B	4
4		ACACGCU/**U**/UUGUGUU	A	1
5	PK19, 24	AAUCACC/**U**/UGAUUUG	B	1
6		AAGAUCA/**U**/AUCUUUA	U	1
7	PK21, 24	CACGCUA/**UUUUU**/AUUGUGU	A	1
8		ACACGCU/**UU**/UUGUGUU	A	2
9		CCGUUAA/**UU**/UUUGAUC	U	1
10		AAUCACC/**UUUA**/UGAUUUG	B	1
11		AAUCACC/**U**/UGAUUUG	B	2
12	wt, 33	AAUCACC/**U**/UGAUUUG	B	1
13	PK14, 33	ACACGCU/**U**/UUGUGUU	A	1
14	PK21, 33	CACGCUA/**UUUUU**/AUUGUGU	A	1
15		AAUCACC/**U**/UGAUUUG	B	1

[a] Nontemplated nucleotide inserts at crossover sites are shown in boldface.
[b] Two types of crossovers were found to have similar flanking sequences, shown as groups A and B separately. Group U includes those crossovers that contain unique sequences at the junction sites.
[c] Defined as the number of independent local lesions accumulating the particular recombinant.

plate switching model predicts that some crossovers occur when the replicase complex approaches or enters heteroduplexes between BMV RNAs (7, 29). The helicase-like domain of 1a protein, which is required for both positive-strand and negative-strand RNA synthesis (23), might influence RNA recombination in several ways. Alteration of a 1a helicase function might directly alter the frequency, location, and/or duration of pausing during RNA synthesis. A possible relationship between pausing, helicase function, and heteroduplex-mediated recombination was articulated in the introduction. This possibility appears consistent with the shift of recombination sites at 33°C with PK19, whose *ts* lesion is adjacent to the putative nucleotide binding site of the helicase-like domain (23).

An indirect way for 1a to influence RNA recombination might be alteration of the interaction between 1a and 2a. Kao et al. (19) demonstrated that the 1a helicase domain binds to the N-terminal sequences of 2a. Mutations within the helicase region may influence 1a-2a binding which, in turn, could affect the overall stability or conformation of the replicase complex, its interaction(s) with the RNA template, or its ability to switch between RNA templates. Conceivably this might influence the incidence of asymmetric crossovers (observed for PK19 and PK21), which may reflect some mechanistic differences from symmetric crossovers. In particular, the observed increase in the frequency of asymmetric junctions (e.g., for PK19 and PK21 at 24°C) is difficult to explain with a conventional heteroduplex mechanism, which assumes that the replicase is being stalled on the RNA1 template by base pairing during negative-strand synthesis (7, 29). The formation of asymmetric crossovers could be explained with a modified heteroduplex mechanism. The latter model assumes that portions of the heteroduplex larger than predicted from the actual crossover sites are being unwound by the replicase complex and that this makes the remote RNA3 sites available for the junctions. Alternatively, it is possible that asymmetric junctions have been formed via a yet unknown mechanism.

Incorporation of nontemplated nucleotides. Observations from other systems suggest that the addition of nontemplated nucleotides is a general phenomenon of viral and nonviral polymerases, including DNA-dependent RNA polymerases and RNA-dependent RNA polymerases (5, 32). Polymerase stuttering, defined as reiterative copying of one or a few adjacent nucleotides, is one possible mechanism of nontemplated addition (5, 8, 25, 32). In BMV, the variable length of an intercistronic oligo(A) tract in RNA3 (3) suggests that BMV replicase is capable of stuttering. Such a mechanism might explain the addition of nontemplated U residues in some cases where one or more templated U's occur on either side of the recombination junction (recombinants 1, 3, 4, 5, 8, 9, 11, 12, 13, and 15 in Table 2). The observation that the nontemplated nucleotides occurred exclusively at the sites of crossovers (Table 2) suggests that incorporation of these residues happened during recombination events. Just as for crossing over itself, altered pausing in the heteroduplex might affect the incidence of nontemplated nucleotide addition, which could occur while the polymerase waits for an opportunity to progress through downstream regions of the template. A role of RNA duplex structure in promoting polymerase stuttering has been demonstrated for the polyadenylation of influenza virus RNA (25). Recombinants 2, 6, 7, and 14 in Table 2 have the nontemplated U's flanked by templated A or C residues. Consequently, in these cases, there are no appropriate template bases at the recombination junctions that the polymerase could repetitively copy to form an oligo(U). Other mechanisms such as a terminal transferase-like activity or some form of RNA editing (10) might be responsible for addition of nontemplated nucleotides in these recombinants.

Besides the effects on the position of recombination sites and in the incorporation of nontemplated nucleotides, an increase in the recombination incidence was observed for infections containing mutant RNA1s (Table 1). This represents another characteristic of recombination which is altered by 1a modifications. This result suggests that the alteration in 1a increases the frequency of crossovers, further supporting a possible relationship between RNA replication and RNA recombination. Possibly a mutated 1a helicase is less efficient in unwinding the heteroduplex structure, causing an increase in template switching. Consistent with this premise is the observation that the effects of mutations PK19 and PK21 on crossover site selection were temperature dependent (as shown in Fig. 3 and 5). In particular, the asymmetry effects induced by these mutations were more pronounced at 24°C than at 33°C, supporting the idea that the proposed structure of the heteroduplex, which is expected to be more stable at lower temperature, influences the position of recombination sites and the effect of 1a mutations.

In summary, our data provide experimental evidence for an interrelationship between RNA replication and at least some recombination events in BMV. Specifically, the observed effects demonstrate that BMV RNA replication protein 1a is involved, directly or indirectly, in recombination between BMV RNA components, possibly because 1a participates in template switching by the replicase. On the basis of these results, additional studies are in progress to further investigate the influence of various viral protein domains, RNA-RNA interactions, and possible duplex unwinding activities on BMV RNA recombination.

ACKNOWLEDGMENTS

We thank Carol Feltz for advice with statistical analysis and Aline Click for technical assistance.

This research was supported by grants from NSF (MCB-9305389) and from NIH (RO1 AI26769) to P.D.N., A.D., and J.J.B. and by grant GM35072 from NIH to P.A.

REFERENCES

1. **Ahlquist, P.** 1992. Bromovirus RNA replication and transcription. Curr. Opin. Genet. Dev. **2:**71–76.
2. **Ahlquist, P., J. Bujarski, P. Kaesberg, and T. C. Hall.** 1984. Localization of the replicase recognition site within brome mosaic virus RNA by hybrid-arrested RNA synthesis. Plant Mol. Biol. **3:**37–44.
3. **Ahlquist, P., R. Dasgupta, and P. Kaesberg.** 1984. Nucleotide sequence of the brome mosaic virus genome and its implications for viral replication. J. Mol. Biol. **172:**369–383.
4. **Allison, R. F., M. Janda, and P. Ahlquist.** 1989. Sequence of cowpea chlorotic mottle virus RNAs 2 and 3 and evidence of a recombination event during bromovirus evolution. Virology **172:**321–330.
5. **Bertholet, C., E. van Meir, B. ten Heggeler-Bordier, and R. Wittek.** 1987. Vaccinia virus produces late mRNAs by discontinuous synthesis. Cell **50:** 153–162.
6. **Bujarski, J. J., and A. M. Dzianott.** 1991. Generation and analysis of nonhomologous RNA-RNA recombinants in brome mosaic virus: sequence complementarities at crossover sites. J. Virol. **65:**4153–4159.
7. **Bujarski, J. J., and P. D. Nagy.** 1994. Targeting of the site of nonhomologous genetic recombination in brome mosaic virus. Arch. Virol. Suppl. **9:**231–238.
8. **Cascone, P. J., C. D. Carpenter, X. H. Li, and A. E. Simon.** 1990. Recombination between satellite RNAs of turnip crinkle virus. EMBO J. **9:**1709–1715.
9. **Cascone, P. J., T. F. Haydar, and A. E. Simon.** 1993. Sequences and structures required for recombination between virus-associated RNAs. Science **260:**801–805.
10. **Cattaneo, R.** 1991. Different types of messenger RNA editing. Annu. Rev. Genet. **25:**71–88.
11. **Dinant, S., M. Janda, P. A. Kroner, and P. Ahlquist.** 1993. Bromovirus RNA replication and transcription require compatibility between the polymerase- and helicase-like viral RNA synthesis proteins. J. Virol. **67:**7181–7189.

12. **Dolja, V. V., and J. C. Carrington.** 1992. Evolution of positive-strand RNA viruses. Semin. Virol. **3:**315–326.
13. **Duncan, D. B.** 1955. Multiple range and multiple F tests. Biometrics **11:**1–42.
14. **Gibbs, A.** 1987. A molecular evolution of viruses: 'trees', 'clocks', and 'modules'. J. Cell Sci. Suppl. **7:**319–337.
15. **Goldbach, R., O. Le Gall, and J. Wellink.** 1991. Alpha-like viruses in plants. Semin. Virol. **2:**19–25.
16. **Gorbalenya, A. E., and E. V. Koonin.** 1989. Viral proteins containing the purine NTP-binding sequence pattern. Nucleic Acids Res. **17:**8413–8440.
17. **Janda, M., R. French, and P. Ahlquist.** 1987. High efficiency T7 polymerase synthesis of infectious RNA from cloned brome mosaic virus cDNA and effects of 5′ extensions of transcript infectivity. Virology **158:**259–262.
18. **Kao, C. C., and P. Ahlquist.** 1992. Identification of the domains required for direct interaction of the helicase-like and polymerase-like RNA replication proteins of brome mosaic virus. J. Virol. **66:**7293–7302.
19. **Kao, C. C., R. Quadt, R. P. Hershberger, and P. Ahlquist.** 1992. Brome mosaic virus RNA replication proteins 1a and 2a form a complex in vitro. J. Virol. **66:**6322–6329.
20. **King, A. M. Q.** 1988. Genetic recombination in positive strand RNA viruses, p. 149–165. *In* E. Domingo, J. J. Holland, and P. Ahlquist (ed.), RNA genetics, vol. 2. CRC Press, Boca Raton, Fla.
21. **Kirkegaard, K., and D. Baltimore.** 1986. The mechanism of RNA recombination in poliovirus. Cell **47:**433–443.
22. **Kroner, P., D. Richards, P. Traynor, and P. Ahlquist.** 1989. Defined mutations in a small region of the brome mosaic virus 2a gene cause diverse temperature-sensitive RNA replication phenotypes. J. Virol. **63:**5302–5309.
23. **Kroner, P. A., B. M. Young, and P. Ahlquist.** 1990. Analysis of the role of brome mosaic virus 1a protein domains in RNA replication, using linker insertion mutagenesis. J. Virol. **64:**6110–6120.
24. **Lai, M. C. M.** 1992. RNA recombination in animal and plant viruses. Microbiol. Rev. **56:**61–79.
25. **Luo, G., W. Luytjes, M. Enami, and P. Palese.** 1991. The polyadenylation signal of influenza virus RNA involves a stretch of uridines followed by the RNA duplex of the panhandle structure. J. Virol. **65:**2861–2867.
26. **Meyers, G., N. Tautz, E. J. Dubovi, and H. J. Thiel.** 1991. Viral cytopathogenicity correlated with integration of ubiquitin-coding sequences. Virology **180:**602–616.
27. **Mise, K., R. F. Allison, M. Janda, and P. Ahlquist.** 1993. Bromovirus movement protein genes play s crucial role in host specificity. J. Virol. **67:**2815–2823.
28. **Nagy, P. D., and J. J. Bujarski.** 1992. Genetic recombination in brome mosaic virus: effect of sequence and replication of RNA on accumulation of recombinants. J. Virol. **66:**6824–6828.
29. **Nagy, P. D., and J. J. Bujarski.** 1993. Targeting the site of RNA-RNA recombination in brome mosaic virus with antisense sequences. Proc. Natl. Acad. Sci. USA **90:**6390–6394.
30. **Romanova, L. I., V. M. Blinov, E. A. Tolskaya, E. G. Viktorova, M. S. Kolesnikova, E. A. Guseva, and V. I. Agol.** 1986. The primary structure of crossover regions of intertypic poliovirus recombinants: a model of recombination between RNA genomes. Virology **155:**202–213.
31. **Strauss, J. H., and E. G. Strauss.** 1988. Evolution of RNA viruses. Annu. Rev. Microbiol. **42:**657–683.
32. **Thomas, S. M., R. A. Lamb, and R. G. Paterson.** 1988. Two mRNAs that differ by two nontemplated nucleotides encode the amino coterminal proteins P and V of the paramyxovirus SV5. Cell **54:**891–902.
33. **Winer, B. J.** 1962. Statistical principles in experimental design, p. 196–198. McGraw-Hill Book Company, New York.
34. **Zimmern, D.** 1988. Evolution of RNA viruses, p 211–240. *In* J. J. Holland, E. Domingo, and P. Ahlquist (ed.), RNA genetics. CRC Press, Boca Raton, Fla.